The Journal of Chemical Physics

Theoretical analysis of selectivity mechanisms in molecular transport through channels and nanopores

Cite as: J. Chem. Phys. **142**, 044705 (2015); https://doi.org/10.1063/1.4906234
Submitted: 31 October 2014 • Accepted: 08 January 2015 • Published Online: 29 January 2015

Shaghayegh Agah, Matteo Pasquali and Anatoly B. Kolomeisky

AIP Publishing

Theoretical analysis of selectivity mechanisms in molecular transport through channels and nanopores

Shaghayegh Agah,[1] Matteo Pasquali,[1,2] and Anatoly B. Kolomeisky[1,2,3,a)]
[1]*Department of Chemical and Biomolecular Engineering, Rice University, Houston, Texas 77005-1892, USA*
[2]*Department of Chemistry, Rice University, Houston, Texas 77005-1892, USA*
[3]*Center for Theoretical Biological Physics, Rice University, Houston, Texas, 77005, USA*

(Received 31 October 2014; accepted 8 January 2015; published online 29 January 2015)

Selectivity is one of the most fundamental concepts in natural sciences, and it is also critically important in various technological, industrial, and medical applications. Although there are many experimental methods that allow to separate molecules, frequently they are expensive and not efficient. Recently, a new method of separation of chemical mixtures based on utilization of channels and nanopores has been proposed and successfully tested in several systems. However, mechanisms of selectivity in the molecular transport during the translocation are still not well understood. Here, we develop a simple theoretical approach to explain the origin of selectivity in molecular fluxes through channels. Our method utilizes discrete-state stochastic models that take into account all relevant chemical transitions and can be solved analytically. More specifically, we analyze channels with one and two binding sites employed for separating mixtures of two types of molecules. The effects of the symmetry and the strength of the molecular-pore interactions are examined. It is found that for one-site binding channels, the differences in the strength of interactions for two species drive the separation. At the same time, in more realistic two-site systems, the symmetry of interaction potential becomes also important. The most efficient separation is predicted when the specific binding site is located near the entrance to the nanopore. In addition, the selectivity is higher for large entrance rates into the channel. It is also found that the molecular transport is more selective for repulsive interactions than for attractive interactions. The physical-chemical origin of the observed phenomena is discussed. [http://dx.doi.org/10.1063/1.4906234]

I. INTRODUCTION

Our understanding of complex processes in chemistry, physics, and biology to a large degree depends on the ability to study individual components of the systems. This requires separation processes, which rely on fundamental concept of *selectivity* that controls how mixtures of different species can be separated based on specific chemical and physical properties of constituent molecules.[1] In addition, separation is one of the most important technological steps in major industrial processes, and it is also relevant for food production and for medicine. Currently, there are many experimental techniques for separations, including chromatography, electrophoresis, distillation, precipitation, and many others.[2] However, in many situations, the majority of them are inefficient, expensive, and unpredictable, especially for mixtures of molecules with very similar chemical properties, or they might even damage the molecules undergoing separation.[2] These observations stimulated a search for new experimental approaches and for better understanding selectivity mechanisms. Transport through channels and pores has been recently proposed as a method for separating molecular mixtures. Several artificial molecular pore systems, which behave similarly to biological channels, have been developed and successfully tested.[4–9] The main idea of this method is to mimic biological systems where very efficient, fast, and robust separations are achieved on a large scale in many cellular systems.[3] However, the theoretical picture of selectivity mechanisms during the molecular transport through nanopores remains unclear. Moreover, we do not understand how biological channels achieve highly efficient separation of molecular mixtures.

Molecular transport through channels is a complex process that involves various physical and chemical interactions between different types of molecules as well as interactions with pores, solvent molecules, and applied external fields. It was investigated theoretically employing various methods.[10–18] In continuum models,[11,12,17] the molecular translocation through the channel is viewed as a one-dimensional diffusion in the effective potential created by a complex network of intermolecular and molecular/pore interactions. Interactions are typically modeled as square-well potentials that occupy the whole volume of the channel, and in most cases, uniform coarse-grained potentials are utilized. These simplifications allow to obtain quantitative results for channel-facilitated molecular transport. A different approach is based on discrete-state stochastic models in which the transport dynamics is analyzed as a set of chemical transitions between specific binding sites in the pore.[13,14,16] Mapping these chemical-kinetic models to a single particle one-dimensional motion along the periodic lattices provides a full dynamic description of the permeation through the pore.[13,14]

a)tolya@rice.edu

Both continuum and discrete-state stochastic methods are closely related to each other.[12] However, it could be argued that the discrete-state stochastic models probably are more convenient for investigating channel-facilitated molecular transport, because the input parameters in these models are chemical rates that can be independently measured in experiments. For the continuum models, the overall effective potentials cannot be obtained so easily from the experiments. These potentials must be approximated or calculated using full atomistic simulations, which currently cannot be done with a high precision.[14]

Surprisingly, there are only few theoretical studies that aim to understand the selectivity mechanisms in the molecular translocation through pores.[16,17] Furthermore, the results obtained in these studies seem to be controversial. Reference 16 argues that the transport of particles that are strongly trapped in the channel is enhanced by the presence of the weakly trapped competing molecules. Similarly, Bauer and Nadler[17] suggest that in the mixtures of molecules that can attractively bind to the pore and inert molecules, the transport of binding species is increased by adding inert molecules to the system. These conclusions are hard to understand. Imagine the situation of very strong attractive interactions for one type of molecules. In this case, the molecules interacting with the channel will be trapped for a long time inside, and varying the amount of the competing molecules will have no effect on dynamics of the system. This discussion suggests that we need a better theoretical analysis of the molecular separation in channel-facilitated transport. In this work, we develop a simple discrete-state stochastic method for analyzing mechanisms of selectivity during the molecular transport through the nanopores. Several theoretical models are solved exactly, providing a full dynamic description of the separation processes and clarifying the physical-chemical foundations of the selectivity mechanisms.

II. THEORETICAL METHOD

To analyze molecular separations during the transport through channels, we consider a system presented in Fig. 1. A mixture of molecules A with a concentration c_A and molecules B with a concentration c_B is moving through a single channel from the left chamber to the right chamber, see Fig. 1(a). Our idea is to view the molecular translocation as an effectively one-dimensional motion along the discrete lattice of binding sites (Fig. 1(b)). There are N binding sites and they correspond to spatial positions inside the channel where molecules reside longer due to stronger interactions with the pore. The molecule A (B) can enter into the channel with the rate $u_0 = k_{on}^A c_A$ ($\alpha_0 = k_{on}^B c_B$), as shown in Fig. 1(b). Inside the nanopore, the molecule A at the binding site j ($j = 1, 2, \ldots, N$) can move forward to the neighboring site $j+1$ with the rate u_j, while the backward transition to the site $j-1$ is taking place with the rate w_j. Similarly, the transition rates for the molecule B from the site j are given by the rates α_j and β_j, respectively, see Fig. 1(b). Every binding site cannot be occupied by more than one particle. To simplify our calculations, we also assume that the concentrations of molecules in the right chamber are zero so that there are no fluxes into the channel from the right, leading to $w_0 = \beta_0 = 0$. It corresponds to the situation when the molecules that already translocated are immediately removed from the system, while the molecular concentrations before the channel are kept constant at all times. Note also that our analysis can be extended for the case when there are finite concentrations of molecules A and B in the right chamber.

To quantify the molecular separation in the nanopore transport, we introduce a new function S that we call a *selectivity parameter*,

$$S = \frac{\frac{J_A}{J_B}}{\frac{c_A}{c_B}}, \tag{1}$$

where J_A and J_B are exit currents from the channel for molecules A and B, respectively. The physical meaning of this parameter is that it gives a relative change in the concentration of exiting molecules in comparison with a composition of the mixture that enters the nanopore. For $S = 1$, there is no separation since the chemical composition of the molecular mixture at the pore exit is the same as in the bulk. $S > 1$ indicates that the mixture exiting the channel is rich in component A. Similarly, $S < 1$ indicates that molecules B are moving preferentially through the pore, and the mixture that exit the channel is richer in the compound B. The selectivity parameter S is a very convenient measure of separation from the experimental point of view because molecular concentrations before and after the nanopore can be easily measured.

A discrete-state stochastic approach provides an explicit framework for evaluating all dynamic properties for molecules translocating through the channel.[13,14] The most important

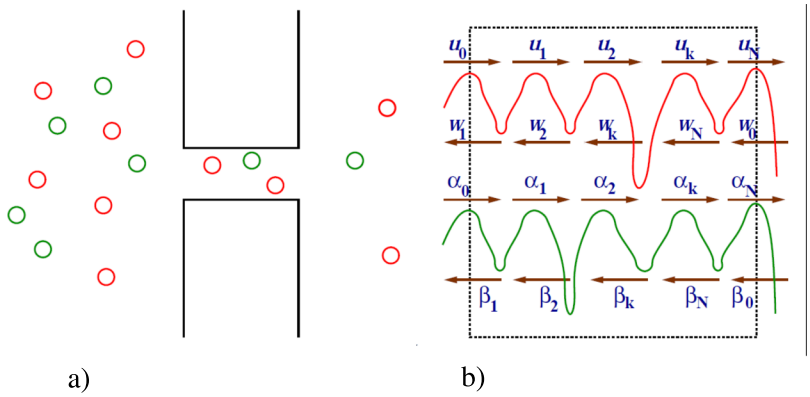

FIG. 1. (a) A schematic view of a molecular transport of a mixture of A (red) and B (green) molecules through a single channel. Particles move from the left chamber to the right chamber. (b) A corresponding discrete-state stochastic model with N binding sites. A dashed box indicates the channel boundaries. Red and green curves describe the free-energy profiles for translocating A and B molecules, respectively.

quantity in this analysis is a probability $P_j^i(t)$ of finding the molecule i ($i = A$ or B) at the binding site j ($j = 1, 2, \ldots, N$) at time t. Its temporal evolution is controlled by a set of master equations, which can be written for the case of no $A-A$, $A-B$, and $B-B$ interactions (including the exclusions) as

$$\frac{dP_j^A(t)}{dt} = u_{j-1}P_{j-1}^A(t) + w_{j+1}P_{j+1}^A(t) - (u_j + w_j)P_j^A(t), \quad (2)$$

for molecules A, and

$$\frac{dP_j^B(t)}{dt} = \alpha_{j-1}P_{j-1}^B(t) + \beta_{j+1}P_{j+1}^B(t) - (\alpha_j + \beta_j)P_j^B(t), \quad (3)$$

for molecules B. In addition, the function

$$P_0(t) \equiv P_{N+1}(t) = 1 - \sum_{j=1}^{N}\left[P_j^A(t) + P_j^B(t)\right] \quad (4)$$

describes a probability to find the nanopore completely empty at time t. It is important to note that for realistic molecular transport with interactions, the expressions are much more complicated. Explicit details of calculations for specific channels are given below.

To investigate the effect of interactions between molecules and channels, we assume that one of the binding sites (say the site k) is different from others. At this site, the molecule A (B) interacts with the nanopore with energy ϵ_A (ϵ_B) stronger than at other binding sites. The case of positive ϵ_i ($i = A$ or B) corresponds to attraction, while for $\epsilon_i < 0$, the channel repels more the molecule A or B at this location. The transition rates into and out of the specific site differ from other binding sites because they must obey the detailed balance conditions.[13,14] It leads to

$$\frac{u'_{k-1}}{w'_k} = \frac{u_{k-1}}{w_k}x_A, \quad \frac{u'_k}{w'_{k+1}} = \frac{u_k}{w_{k+1}}\frac{1}{x_A}, \quad (5)$$

for the molecule A, where

$$x_A = \exp(\beta\epsilon_A). \quad (6)$$

Here, the transition rates u_{k-1}, u_k, w_k, and w_{k+1} describe the uniform channel without specific interactions ($\epsilon_A = \epsilon_B = 0$), while u'_{k-1}, u'_k, w'_k, and w'_{k+1} are real transition rates for $\epsilon_A \neq 0$ and $\epsilon_B \neq 0$. To describe dynamics of the system, we need explicit expressions for all rates and it can be shown that[13,14]

$$u'_{k-1} = u_{k-1}x_A^{\theta}, \quad u'_k = u_k x_A^{\theta-1}, \quad w'_k = w_k x_A^{\theta-1}, \quad w'_{k+1} = w_{k+1}x_A^{\theta}, \quad (7)$$

where the parameter $0 \le \theta \le 1$ describes the change in transitions rates due to the interaction energy ϵ_A. It has a physical meaning of the relative distance to a transition state for each chemical process.[13,14] Generally, the parameter θ might depend on the interaction energies, but to simplify calculations, we assume that it is a constant.

Similar analysis can be done for the molecules B. The detailed balance condition at the specific site reads as

$$\frac{\alpha'_{k-1}}{\beta'_k} = \frac{\alpha_{k-1}}{\beta_k}x_B, \quad \frac{\alpha'_k}{\beta'_{k+1}} = \frac{\alpha_k}{\beta_{k+1}}\frac{1}{x_B}, \quad (8)$$

with

$$x_B = \exp(\beta\epsilon_B). \quad (9)$$

The transition rates into and out of the specific site for molecules B are given by

$$\alpha'_{k-1} = \alpha_{k-1}x_B^{\theta}, \quad \alpha'_k = \alpha_k x_B^{\theta-1}, \quad \beta'_k = \beta_k x_B^{\theta-1}, \quad \beta'_{k+1} = \beta_{k+1}x_B^{\theta}. \quad (10)$$

Here, for simplicity, we assume that the coefficient θ is the same for both molecules A and B. Our calculations can be expanded to account for different parameters θ. But the physical picture of the separation most probably does not depend on this, and we choose the simplest case in order explain better the selectivity mechanisms.

In the discrete-state models for the transport in the channel with N binding sites, the number of different molecular configurations is 3^N because each site can be found in one of three possible states: it can be occupied by the molecule A, molecule B, or it can be empty. It is difficult to solve this problem for arbitrary N. However, we can obtain exact analytical solutions for small $N = 1$ and $N = 2$. It allows us to understand better molecular separation in the nanopores.

A. Channels with one binding site

We start our theoretical analysis by considering the simplest model with only one binding site in the channel, i.e., with $N = 1$. There are three possible states in the system. We define probabilities to find the pore occupied by the molecule A, by the molecule B, or to be empty at time t as $P^A(t)$, $P^B(t)$, or $P^0(t)$, respectively. The corresponding kinetic scheme for the system is shown in Fig. 2. To simplify calculations, let us assume that the entrance rate constants for both types of molecules are the same, $k_{on}^A = k_{on}^B \equiv k_{on}$. It corresponds to the situation when these molecules are similar in their chemical nature. This means that there is a certain type of similarity that gives comparable entrance rates but different interactions with the channel. In addition, we take $u_k = w_k = \alpha_k = \beta_k \equiv u$, which means that the transition rates inside the uniform channels

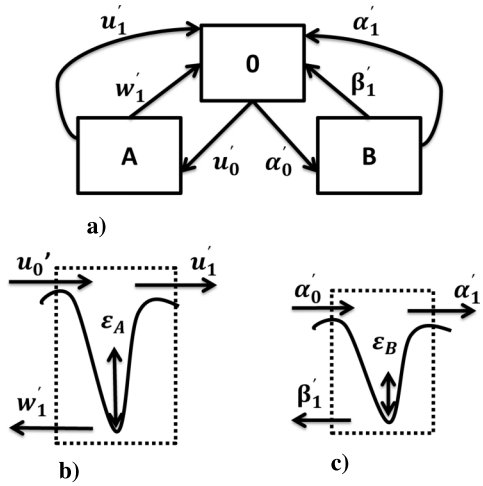

FIG. 2. A discrete-state stochastic model for a transport of a molecular mixture across a channel with one binding site. (a) An effective free-energy landscape for translocation of molecules A. (b) An effective free-energy landscape for translocation of molecules B. (c) A kinetic scheme for the model. Boxes describe different states of the channel, while arrows show possible transitions between states.

(when $\epsilon_A = \epsilon_B = 0$) in both directions are the same for both molecules A and B. Then, the specific values of transition rates in this model are given by

$$u_0' = k_{on} c_A x_A^{\theta}, \quad u_1' = u x_A^{\theta-1}, \quad w_1' = u x_A^{\theta-1} \tag{11}$$

and

$$\alpha_0' = k_{on} c_B x_B^{\theta}, \quad \alpha_1' = u x_B^{\theta-1}, \quad \beta_1' = u x_B^{\theta-1}. \tag{12}$$

Since the channel might be found in one of three different configurations, its dynamics is governed by a set of three master equations,

$$\frac{dP^0(t)}{dt} = (u_1' + w_1')P^A(t) + (\alpha_1' + \beta_1')P^B(t) - (u_0' + \alpha_0')P^0(t), \tag{13}$$

$$\frac{dP^A(t)}{dt} = u_0' P^0(t) - (u_1' + w_1')P^A(t), \tag{14}$$

$$\frac{dP^B(t)}{dt} = \alpha_0' P^0(t) - (\alpha_1' + \beta_1')P^B(t). \tag{15}$$

This set of equations obeys the normalization condition $P^A(t) + P^B(t) + P^0(t) = 1$ at all times. We are interested in the stationary-state properties of the system when $\frac{dP^i(t)}{dt} = 0$ for $i = A$, B, or 0. Then, these master equations can be solved to produce the steady-state probabilities of different channel configurations,

$$P^0 = \frac{(u_1' + w_1')(\alpha_1' + \beta_1')}{(u_1' + w_1')(\alpha_1' + \beta_1') + u_0'(\alpha_1' + \beta_1') + \alpha_0'(u_1' + w_1')}, \tag{16}$$

$$P^A = \frac{u_0'(\alpha_1' + \beta_1')}{(u_1' + w_1')(\alpha_1' + \beta_1') + u_0'(\alpha_1' + \beta_1') + \alpha_0'(u_1' + w_1')}, \tag{17}$$

$$P^B = \frac{\alpha_0'(u_1' + w_1')}{(u_1' + w_1')(\alpha_1' + \beta_1') + u_0'(\alpha_1' + \beta_1') + \alpha_0'(u_1' + w_1')}. \tag{18}$$

After applying Eqs. (11) and (12), these expressions can be simplified into

$$P^0 = \frac{2u}{2u + k_{on}(c_A x_A + c_B x_B)}, \tag{19}$$

$$P^A = \frac{k_{on} c_A x_A}{2u + k_{on}(c_A x_A + c_B x_B)}, \tag{20}$$

$$P^B = \frac{k_{on} c_B x_B}{2u + k_{on}(c_A x_A + c_B x_B)}. \tag{21}$$

One can see that for large entrance rates ($k_{on}c_A, k_{on}c_B \gg u$), the probability to find the channel occupied is high, while for large exiting rates ($u \gg k_{on}c_A$, $k_{on}c_B$), it is usually empty.

To evaluate the effectiveness of the separation in this system requires the stationary-state fluxes for A and B,

$$J_A = u_0' P^0 = u_1' P^A, \quad J_B = \alpha_0' P^0 = \alpha_1' P^B. \tag{22}$$

Employing Eqs. (19)-(21), the molecular fluxes are

$$J_A = \frac{u k_{on} c_A x_A^{\theta}}{2u + k_{on}(c_A x_A + c_B x_B)}, \quad J_B = \frac{u k_{on} c_B x_B^{\theta}}{2u + k_{on}(c_A x_A + c_B x_B)}. \tag{23}$$

The selectivity parameter is

$$S = \frac{\frac{J_A}{J_B}}{\frac{c_A}{c_B}} = \left(\frac{x_A}{x_B}\right)^{\theta} = \exp(\beta\theta\Delta\epsilon), \tag{24}$$

where $\Delta\epsilon = \epsilon_A - \epsilon_B$. Clearly, that in this model, the selectivity is fully controlled by the difference in molecule/pore interactions. The larger the difference, the better separation might be achieved. In addition, it also depends on the parameter θ. The selectivity is very sensitive to interactions for $\theta \to 1$, while for $\theta = 0$, there will be no separation. These observations can be explained if we notice that for $\theta = 1$, the exiting rates from the channel are the same for both types of molecules, as shown in Eqs. (11) and (12), while the entrance rates are strongly influenced by interactions. At the same time, for $\theta = 0$, the ratio of the particles current through the system is not affected by the interactions as one might conclude from Eq. (22).

This theoretical method is also useful for understanding of how the presence of one type of molecules influences the dynamics of other type of molecules. Suppose, we do not have molecules B in our mixture, i.e., $c_B = 0$. Then, the molecular flux for particles A is equal to

$$J_A(c_B = 0) = \frac{u k_{on} c_A x_A^{\theta}}{2u + k_{on} c_A x_A}. \tag{25}$$

Comparing with Eq. (23), we conclude that

$$\frac{J_A(c_B = 0)}{J_A} = \frac{2u + k_{on}(c_A x_A + c_B x_B)}{2u + k_{on} c_A x_A} > 1. \tag{26}$$

This is an important result since it indicates that adding the molecules B to the system *always* lowers the flux of the molecules A. This is because it increases the probability for the pore to be occupied by any particle, which obviously decreases the entering molecular flux of particles A.

B. Channels with two binding sites

A more realistic situation is when channels have more than one binding site so that multiple species can be found simultaneously in the nanopore. To model these systems, we analyze a channel with two binding sites ($N = 2$), as shown in Fig. 3. In this case, dynamic properties depend on which site has specific interactions between the molecules and the pore. Let us start with the case when the second site (near the exit) is a specific one. We again assume that the entrance rate constants for both species are the same, $k_{on}^A = k_{on}^B \equiv k_{on}$. Also, we take the exit rates back to the left chamber to be the

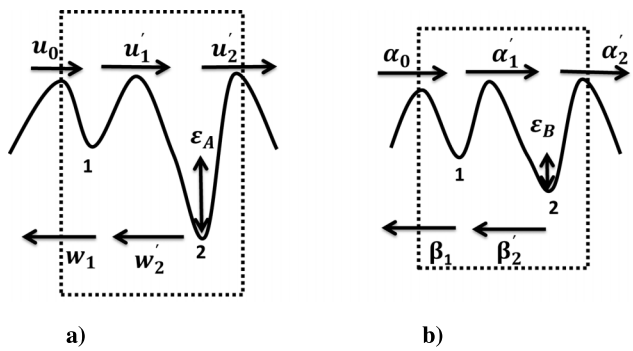

FIG. 3. A discrete-state stochastic model for a transport of a molecular mixture across a channel with two binding sites. Special site is near the exit. (a) The free-energy profile for translocation of A molecules. (b) The free-energy profile for translocation of B molecules.

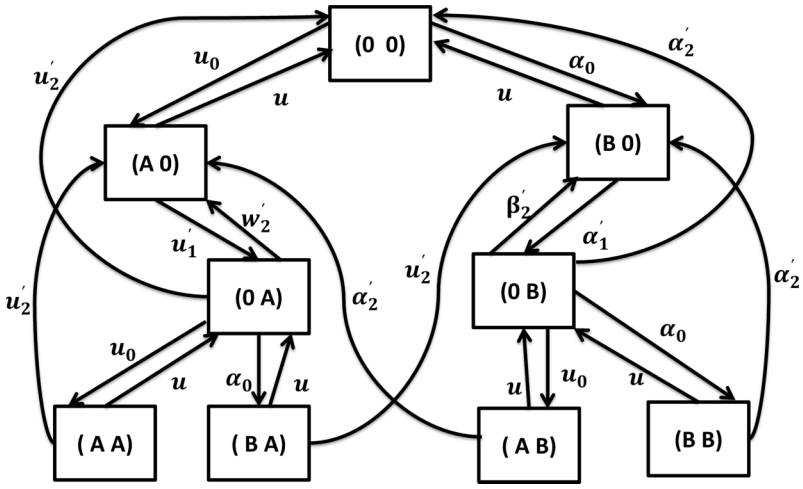

FIG. 4. A kinetic scheme for the nanopore with two binding sites where the second site is special. Boxes describe different states of the channel, while arrows show possible transitions between states.

same, i.e., $w_1 = \beta_1 = u$. The transition rates into and out of the specific site can be written as

$$u_1' = ux_A^{\theta}, \quad u_2' = ux_A^{\theta-1}, \quad w_2' = ux_A^{\theta-1} \tag{27}$$

and

$$\alpha_1' = ux_B^{\theta}, \quad \alpha_2' = ux_B^{\theta-1}, \quad \beta_2' = ux_B^{\theta-1}. \tag{28}$$

The entrance rates are given by

$$u_0 = k_{on}c_A, \quad \alpha_0 = k_{on}c_B. \tag{29}$$

In the channel with two binding sites, there are 9 possible states depending on the occupancy and we label them as (i, j) for $i, j = A$, B, or 0. The kinetic scheme with all possible transitions is presented in Fig. 4. We introduce probability functions $P(i, j; t)$ of finding the nanopore in the state (i, j) at time t ($i, j = 0$, A, or B). In order to fully describe the dynamics of the system at long times, we solve the corresponding master equation in the limit of $t \to \infty$ (see Appendix for details).

The molecular fluxes are

$$J_A = u_2'[P(0, A) + P(A, A) + P(B, A)], \tag{30}$$

and

$$J_B = \alpha_2'[P(0, B) + P(B, B) + P(A, B)]. \tag{31}$$

Then, the current for molecules A is

$$J_A = ux_A^{\theta-1}\left[1 + \frac{k_{on}(c_A + c_B)}{u(1 + x_A^{\theta-1})}\right]P(0, A), \tag{32}$$

while for molecules B, it is

$$J_B = ux_B^{\theta-1}\left[1 + \frac{k_{on}(c_A + c_B)}{u(1 + x_B^{\theta-1})}\right]P(0, B). \tag{33}$$

From the detailed calculations in the Appendix, we derive that

$$\frac{P(0, A)}{P(0, B)} = \frac{c_A}{c_B}\frac{\frac{1+x_B^{\theta}}{x_B+x_B^{\theta}} + \frac{u(2/x_B+x_B^{\theta-1})}{k_{on}(c_A+c_B)}}{\frac{1+x_A^{\theta}}{x_A+x_A^{\theta}} + \frac{u(2/x_A+x_A^{\theta-1})}{k_{on}(c_A+c_B)}}. \tag{34}$$

Then, the expression for the selectivity parameter for $N = 2$ model with the specific site at $i = 2$, which we label as S_2, is given by

$$S_2 = \left(\frac{x_A}{x_B}\right)^{\theta}\left[\frac{k_{on}(c_A + c_B) + u(1 + x_A^{\theta-1})}{k_{on}(c_A + c_B) + u(1 + x_B^{\theta-1})}\right] \times \left[\frac{k_{on}(c_A + c_B)(1 + x_B^{\theta}) + u(1 + x_B^{\theta-1})(2 + x_B^{\theta})}{k_{on}(c_A + c_B)(1 + x_A^{\theta}) + u(1 + x_A^{\theta-1})(2 + x_A^{\theta})}\right]. \tag{35}$$

Comparing Eqs. (24) and (35), one can clearly see that in the channel with two binding sites, in contrast to the single-site channel, the selectivity is not determined only by interactions between the molecules and the pore. It is interesting to consider the situation when both molecules strongly attract to the pore, $x_A \gg 1$ and $x_B \gg 1$. Then, Eq. (34) gives us

$$\frac{P(0, A)}{P(0, B)} \simeq \frac{c_A}{c_B}\left(\frac{x_B}{x_A}\right)^{\theta-1}, \tag{36}$$

which leads to a surprising conclusion that in this limit, the molecular transport is not selective at all, $S_2 \simeq 1$. It can be understood by noting that the second specific site is always occupied by molecules. The stronger the attraction for the species A, the more probable to find them at this site in comparison with the species B. But the rate out of this site is inversely proportional to the strength of the interaction. As a result of this compensation effect, the particle current for both type of molecules is the same [see Eqs. (32) and (33)] and the separation cannot be achieved. A different situation is observed for strong repulsions ($x_A \ll 1$ and $x_B \ll 1$). In this case, the selectivity parameter is given by

$$S_2 \simeq \left(\frac{x_A}{x_B}\right)^{\theta}, \tag{37}$$

which suggests a very efficient separation during the molecular translocation through the channel. Thus, selectivity mechanisms work better for repulsive interactions between the molecules and the pore.

We can also investigate the effect of the entrance rates on selectivity. For high entrance rates, $k_{on}(c_A + c_B) \gg u$, the expression for the selectivity parameter is quite simple,

$$S_2 \simeq \left(\frac{x_A}{x_B}\right)^{\theta}\frac{1 + x_B^{\theta}}{1 + x_A^{\theta}}. \tag{38}$$

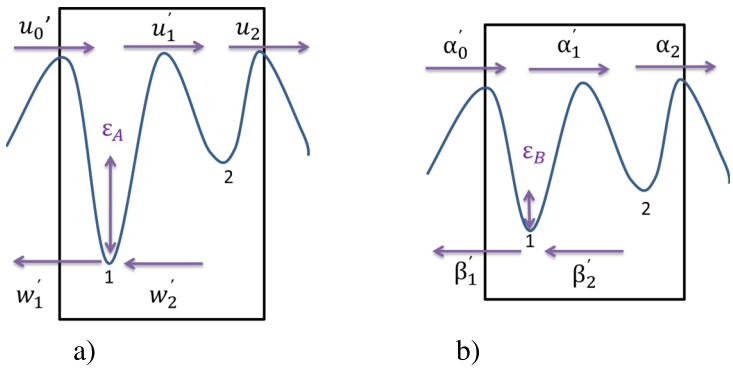

FIG. 5. The selectivity parameter as a function of the difference in molecular interactions with the pore for the channel with $N = 2$ binding sites. The second binding site is the specific one. Here, we define $u_0 = k_{on}c_A = k_{on}c_B$ as the entrance rate into the channel. The following parameters were used in calculations: $\theta = 0.5$, $c_A = c_B$, and $\epsilon_B = 0$.

In the opposite limit of low entrance rates, $k_{on}(c_A + c_B) \ll u$, surprisingly, the expression is only slightly different,

$$S_2 \simeq \left(\frac{x_A}{x_B}\right)^{\theta} \frac{2 + x_B^{\theta}}{2 + x_A^{\theta}}. \tag{39}$$

These results suggest that changing the concentration of molecules before the channel and/or entrance rate constants does not affect much the selectivity. This is because the main events are taking place at the second site which is not close to the entrance.

It is also useful to consider the case of $\epsilon_B = 0$, i.e., $x_B = 1$. The selectivity parameter is equal then to

$$S_2 = x_A^{\theta}\left[\frac{k_{on}(c_A + c_B) + u(1 + x_A^{\theta-1})}{k_{on}(c_A + c_B) + 2u}\right] \times \left[\frac{2k_{on}(c_A + c_B) + 6u}{k_{on}(c_A + c_B)(1 + x_A^{\theta}) + u(1 + x_A^{\theta-1})(2 + x_A^{\theta})}\right], \tag{40}$$

and it is presented in Fig. 5 for high and low entrance rates. We can see that for the repulsion between the molecule A and the pore, the separation is quite efficient for all possible entrance rates. In this case, the passing through the second site is a rate-limiting step for the molecules A, which does not depend on how fast they entered the channel. For attractive interactions between the molecules A and the pore, the selectivity is not so efficient. It can be derived from Eq. (40) that $2 \le S_2 \le 3$. The modest separation values can be explained using the same compensation mechanism as we argued above. The selectivity parameter S_2 is slightly larger for smaller entrance rates because in this case, the relative flux of molecules A is also slightly larger than the flux of the molecules B as one might conclude from Eqs. (32) and (33).

Now, let us analyze a channel with two binding sites where specific interactions are taking place in the first site, near the entrance. Fig. 6 shows the free-energy profiles for translocation of molecules A and B via such nanopore. As before, the entrance rate constants for both species are taken to be the same, $k_{on}^A = k_{on}^B \equiv k_{on}$. We also assume that the exit rates into the right chamber are the same for both type of particles, i.e., $u_2 = \alpha_2 = u$. Transitions into and out of the special site are modified as compared with dynamics in the uniform channel. The corresponding transition rates are obtained using the detailed balance arguments and they are given by

$$u_0' = k_{on}c_A x_A^{\theta}, \quad u_1' = u x_A^{\theta-1}, w_1' = u x_A^{\theta-1}, w_2' = u x_A^{\theta} \tag{41}$$

and

$$\alpha_0' = k_{on}c_B x_B^{\theta}, \quad \alpha_1' = u x_B^{\theta-1}, \beta_1' = u x_B^{\theta-1}, \beta_2' = u x_A^{\theta}. \tag{42}$$

Depending on the occupation of the bindings sites, the channel can be found in one of 9 possible configurations (i, j) (for $i, j = 0$, A, or B). Each of them is specified by the probability functions $P(i, j; t)$. The overall kinetic scheme for this model is presented in Fig. 7. Again, we are interested in the long-time dynamics of the system which can be obtained after solving the corresponding master equations at $t \to \infty$ and obtaining the stationary-state probability functions $P(i, j)$ $(i, j = 0$, A, or $B)$. The details of the calculations are given in the Appendix.

The particle currents in this model can be written as

$$J_A = u_1' P(A, 0) - w_2' P(0, A) \tag{43}$$

for the molecules A, while for the molecules B, we have

$$J_B = \alpha_1' P(B, 0) - \beta_2' P(0, B). \tag{44}$$

As shown in the Appendix, these molecular fluxes are equal to

$$J_A = u\left[1 + \frac{k_{on}c_B x_B^{\theta}}{u(1 + x_B^{\theta-1})} + \frac{k_{on}c_A x_A^{\theta}}{u(1 + x_A^{\theta-1})}\right] P(0, A) \tag{45}$$

for molecules A and

$$J_B = u\left[1 + \frac{k_{on}c_B x_B^{\theta}}{u(1 + x_B^{\theta-1})} + \frac{k_{on}c_A x_A^{\theta}}{u(1 + x_A^{\theta-1})}\right] P(0, B) \tag{46}$$

for molecules B. In addition, it can be found that

$$\frac{P(0, A)}{P(0, B)} = \frac{c_A}{c_B} \frac{\left[1 + \frac{2}{x_B^{\theta}}\left(1 + \frac{k_{on}c_B x_B^{\theta}}{u(1 + x_B^{\theta-1})} + \frac{k_{on}c_A x_A^{\theta}}{u(1 + x_A^{\theta-1})}\right) + \frac{k_{on}c_B(x_B^{\theta-1} - x_A^{\theta-1})}{u(1 + x_B^{\theta-1})(1 + x_A^{\theta-1})}\right]}{\left[1 + \frac{2}{x_A^{\theta}}\left(1 + \frac{k_{on}c_B x_B^{\theta}}{u(1 + x_B^{\theta-1})} + \frac{k_{on}c_A x_A^{\theta}}{u(1 + x_A^{\theta-1})}\right) + \frac{k_{on}c_A(x_A^{\theta-1} - x_B^{\theta-1})}{u(1 + x_B^{\theta-1})(1 + x_A^{\theta-1})}\right]}. \tag{47}$$

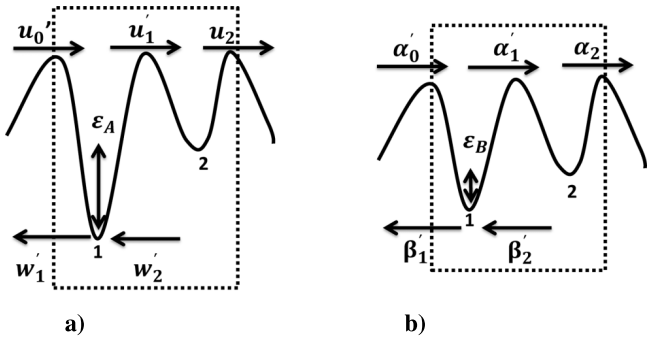

FIG. 6. A discrete-state stochastic model for a transport of a molecular mixture across a channel with two binding sites. The specific site is near the entrance. (a) The free-energy profile for translocation of A molecules. (b) The free-energy profile for translocation of B molecules.

The selectivity parameter for $N = 2$ channel with the specific site at the entrance, S_1, is given by

$$S_1 = \frac{J_A/J_B}{c_A/c_B} = \frac{P(0,A)}{P(0,B)}\frac{c_B}{c_A}, \tag{48}$$

which from Eq. (47) produces the final expression,

$$S_1 = \frac{\left[1+\frac{2}{x_B^\theta}\left(1+\frac{k_{on}c_Bx_B^\theta}{u(1+x_B^{\theta-1})}+\frac{k_{on}c_Ax_A^\theta}{u(1+x_A^{\theta-1})}\right)+\frac{k_{on}c_B(x_B^{\theta-1}-x_A^{\theta-1})}{u(1+x_B^{\theta-1})(1+x_A^{\theta-1})}\right]}{\left[1+\frac{2}{x_A^\theta}\left(1+\frac{k_{on}c_Bx_B^\theta}{u(1+x_B^{\theta-1})}+\frac{k_{on}c_Ax_A^\theta}{u(1+x_A^{\theta-1})}\right)+\frac{k_{on}c_A(x_A^{\theta-1}-x_B^{\theta-1})}{u(1+x_B^{\theta-1})(1+x_A^{\theta-1})}\right]}. \tag{49}$$

One can see that this expression is different from the selectivity parameter S_2 as given by Eq. (35). It leads us to an important conclusion that a symmetry of molecular interactions with the pore influences the selectivity mechanisms in the transport through channels.

For strong positive attractive interactions for both molecules ($x_A \gg 1$ and $x_B \gg 1$), the selectivity parameter S_1 simplifies into

$$S_1 \simeq \frac{1+\frac{2k_{on}c_B}{u}+\frac{2k_{on}c_A}{u}\left(\frac{x_A}{x_B}\right)^\theta}{1+\frac{2k_{on}c_A}{u}+\frac{2k_{on}c_B}{u}\left(\frac{x_B}{x_A}\right)^\theta}. \tag{50}$$

The analysis of this equation suggests that in this case, the separation is not efficient at low entrance rates. For large entrance rates, it becomes

$$S_1 \simeq \frac{c_B + c_A\left(\frac{x_A}{x_B}\right)^\theta}{c_A + c_B\left(\frac{x_B}{x_A}\right)^\theta}. \tag{51}$$

In the opposite limit of strong repulsions ($x_A \to 0$ and $x_B \to 0$), we obtain

$$S_1 \simeq \left(\frac{x_A}{x_B}\right)^\theta. \tag{52}$$

It means that in this case, the selectivity mechanisms are quite efficient and they are fully dominated by the difference in interactions between molecules and pores.

It is instructive also to consider a situation when there is no additional interactions for molecules B ($\epsilon_B = 0$ and $x_B = 1$). In this case, the selectivity parameter can be written as

$$S_1 = \frac{\left[1+2\left(1+\frac{k_{on}c_B}{2u}+\frac{k_{on}c_Ax_A^\theta}{u(1+x_A^{\theta-1})}\right)+\frac{k_{on}c_B(1-x_A^{\theta-1})}{2u(1+x_A^{\theta-1})}\right]}{\left[1+\frac{2}{x_A^\theta}\left(1+\frac{k_{on}c_B}{2u}+\frac{k_{on}c_Ax_A^\theta}{u(1+x_A^{\theta-1})}\right)+\frac{k_{on}c_A(x_A^{\theta-1}-1)}{2u(1+x_A^{\theta-1})}\right]}. \tag{53}$$

The results of S_1 as a function of the molecular interactions with the pore for various entrance rates are presented in Fig. 8. The molecular separation is efficient for repulsive interactions (for molecules A) for all ranges of entrance rates. However, for attractive interactions, the selectivity mechanisms work better for larger entrance rates because the first site in the channel is the location of strong interactions, and the relative increase in the entrance rate for molecules A is much larger.

Our calculations indicate that the symmetry of the molecular/pore interactions is the important factor in the separation processes. Let us analyze this observation in more detail by comparing the selectivity parameters for $N = 2$ channels with different location of the specific sites. This would correspond to varying the symmetry of interaction potential. The results are presented in Figs. 9 and 10. At repulsive interactions, the molecular separations are equally effective for all ranges of the entrance rates independently of the location of the specific site. However, the behavior is very different for attractive interactions. The selectivity parameter

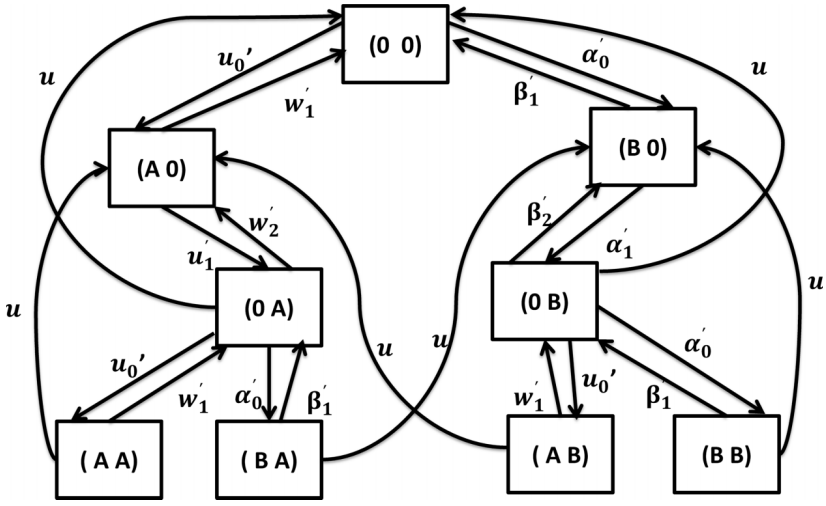

FIG. 7. A kinetic scheme for the nanopore with two binding sites where the first site is specific. Boxes describe different states of the channel, while arrows show possible transitions between states.

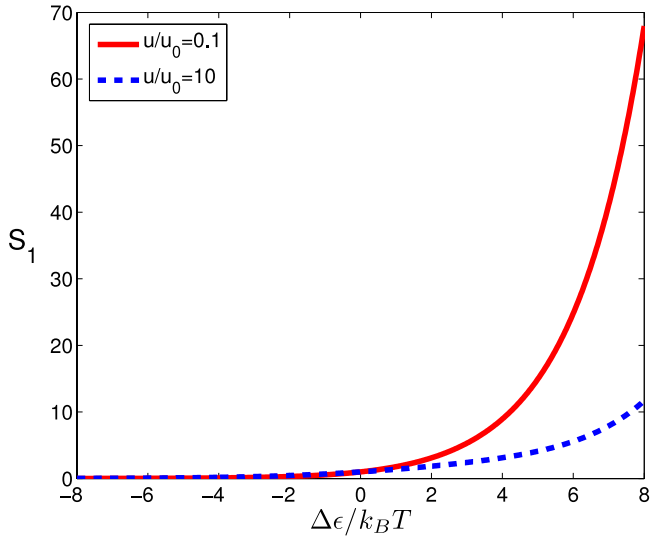

FIG. 8. The selectivity parameter as a function of the difference in molecular interactions with the pore for the channel with $N = 2$ binding sites. The first binding site is a specific one. Here, we define $u_0 = k_{on}c_A = k_{on}c_B$ as the entrance rate into the channel. The following parameters were used in calculations: $\theta = 0.5$, $c_A = c_B$, and $\epsilon_B = 0$.

S_1 grows without a bound, while S_2 reaches a saturation, and $S_1 \gg S_2$ for large positive interactions. It means that the selectivity mechanisms are very effective when the specific site is near the entrance and the efficiency is not high when the specific site is near the exit. In addition, the most efficient separations can be achieved for high entrance rates into the nanopore. These observation can be understood using the following arguments. For the channel with the specific site near the exit, increasing the strength of interaction with the molecules A will not increase their flux if there is a molecule B in the first site. But for the nanopore with the specific site near the entrance, such increase will definitely accelerate the entrance of molecules A into the channel because both molecules can enter *independently* of each other. This effect is stronger for larger entrance rates.

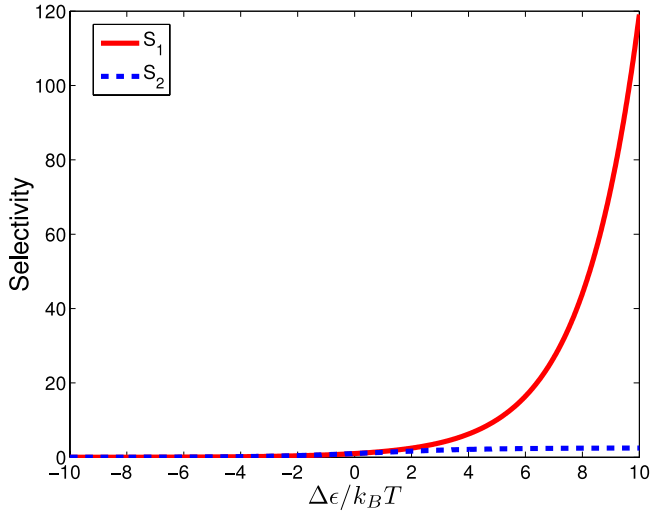

FIG. 9. Comparison of selectivity parameters as a function of the interaction strength for varying potential symmetry at large entrance rates. Parameters used in calculations are $\theta = 0.5$, $c_A = c_B$, $u/u_0 = 0.1$, and $\epsilon_B = 0$.

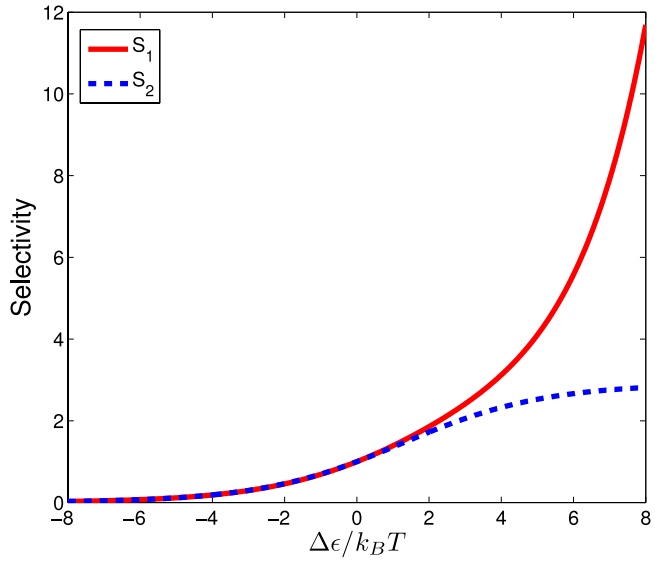

FIG. 10. Comparison of selectivity parameters as a function of the interaction strength for varying potential symmetry at low entrance rates. Parameters used in calculations are $\theta = 0.5$, $c_A = c_B$, $u/u_0 = 10$, and $\epsilon_B = 0$.

III. SUMMARY AND CONCLUSIONS

We developed a theoretical framework for analyzing selectivity mechanisms in the molecular transport through the channels. Our approach employs discrete-state stochastic models that view the translocation as a set of chemical transitions between binding sites in the pore. Because these models can be solved analytically, it allows us to investigate the microscopic origin of separation processes during the translocation via channels.

More specifically, we analyzed selectivity mechanisms in nanopores with one and two binding sites at stationary-state conditions. Our calculations indicate that the strength of molecular interactions and the symmetry of interaction potentials are main factors that govern the molecular selectivity processes. It is found that adding the second type of molecules to the system always decreases the flux of the first type of molecules. For one-site channels, only the strength of interactions is important in driving the separation, while for more realistic two-site channels, the symmetry also starts to play an important role. We find that the selectivity is very efficient for repulsive interactions. For attractions, the dynamics is different depending on the position of the specific binding site. The molecular separation is fast and efficient when stronger attractions are found at the site near the entrance, while it shows a saturating behavior as a function of the interaction strength when the special binding sites is near the exit. We argue that this result is due to the fact that the entrance rates are affected stronger when the specific site is near the entrance. It is also found that selectivity is more efficient for large entrance rates. Our analysis illustrates the fundamental connection between the potential symmetry and the strength of interactions in the channel-facilitated molecular separation phenomena.

The main advantage of our approach is the ability to explicitly evaluate all dynamic properties in the molecular transport via nanopores. This allows us to provide clear

physical-chemical explanations of these complex phenomena. However, it is important to note that our analytical method is limited by the small number of binding sites in the channel because the number of equations in the system scales exponentially with the number of the binding sites. In addition, our method neglects many realistic features of the channel transport, such as intermolecular interactions, molecules passing over each other, conformational changes in molecules and pores, that might strongly affect selectivity mechanisms. It will be important to compare our approach with more advanced theoretical and computational methods, as well as to test it in experimental systems.

ACKNOWLEDGMENTS

This work was supported by grants from the Welch Foundation (C-1559 and C-1668).

APPENDIX: DETAILED CALCULATIONS FOR CHANNELS WITH $N = 2$ BINDING SITES

In this Appendix, we present detailed derivations of the equations and relations used in the main text for the molecular separations in two-site nanopores.

1. $N = 2$ channels: The special site is at the exit

The dynamics of this system is governed by master equations for temporal evolution of the probabilities functions $P(i,j;t)$ $(i,j = 0, A \text{ or } B)$,

$$\frac{dP(0,0;t)}{dt} = u_2'P(0,A;t) + \alpha_2'P(0,B;t) + u[P(A,0;t) + P(B,0;t)] - (u_0+\alpha_0)P(0,0;t), \tag{A1}$$

$$\frac{dP(A,0;t)}{dt} = u_0P(0,0;t) + u_2'P(A,A;t) + w_2'P(0,A;t) + \alpha_2'P(A,B;t) - (u_1'+u)P(A,0;t), \tag{A2}$$

$$\frac{dP(B,0;t)}{dt} = \alpha_0P(0,0;t) + \alpha_2'P(B,B;t) + \beta_2'P(0,B;t) + u_2'P(B,A;t) - (\alpha_1'+u)P(B,0;t), \tag{A3}$$

$$\frac{dP(0,A;t)}{dt} = u_1'P(A,0;t) + u[P(A,A;t) + P(B,A;t)] - (u_0+\alpha_0+w_2'+u_2')P(0,A;t), \tag{A4}$$

$$\frac{dP(0,B;t)}{dt} = \alpha_1'P(B,0;t) + u[P(B,B;t) + P(A,B;t)] - (u_0+\alpha_0+\beta_2'+\alpha_2')P(0,B;t), \tag{A5}$$

$$\frac{dP(A,A;t)}{dt} = u_0P(0,A;t) - (u+u_2')P(A,A;t), \tag{A6}$$

$$\frac{dP(B,A;t)}{dt} = \alpha_0P(0,A;t) - (u+u_2')P(B,A;t), \tag{A7}$$

$$\frac{dP(A,B;t)}{dt} = u_0P(0,B;t) - (u+\alpha_2')P(A,B;t), \tag{A8}$$

$$\frac{dP(B,B;t)}{dt} = \alpha_0P(0,B;t) - (u+\alpha_2')P(B,B;t). \tag{A9}$$

In addition, we have a normalization condition,

$$P(0,0;t) + P(A,0;t) + P(B,0;t) + P(0,A;t) + P(0,B;t) + P(A,A;t) + P(B,A;t) + P(A,B;t) + P(B,B;t) = 1. \tag{A10}$$

At large times, the system reaches the stationary state, and we derive from Eqs. (A6)–(A9),

$$P(A,B) = \frac{u_0}{u+\alpha_2'}P(0,B), \quad P(B,A) = \frac{\alpha_0}{u+u_2'}P(0,A),$$
$$P(A,A) = \frac{u_0}{u+u_2'}P(0,A), \quad P(B,B) = \frac{\alpha_0}{u+\alpha_2'}P(0,B). \tag{A11}$$

Then, substituting these expressions into Eqs. (A2) and (A3), we obtain

$$P(A,0) = \left[\frac{u_2'(u_0+\alpha_0)}{u_1'(u+u_2')} + \frac{u_2'+w_2'}{u_1'}\right]P(0,A) \tag{A12}$$

and

$$P(B,0) = \left[\frac{\alpha_2'(u_0+\alpha_0)}{\alpha_1'(u+\alpha_2')} + \frac{\alpha_2'+\beta_2'}{\alpha_1'}\right]P(0,B). \tag{A13}$$

At the same time, Eq. (A1) yields the following expression:

$$P(0,0) = \left[\frac{u(u_2'+w_2')+u_1'u_2'}{u_1'(u_0+\alpha_0)} + \frac{uu_2'}{u_1'(u+u_2')}\right]P(0,A) + \left[\frac{u(\alpha_2'+\beta_2')+\alpha_1'\alpha_2'}{\alpha_1'(u_0+\alpha_0)} + \frac{u\alpha_2'}{\alpha_1'(u+\alpha_2')}\right]P(0,B). \tag{A14}$$

Now, with the help of Eq. (A11), we can rewrite the particle currents in Eqs. (30) and (31) in the following form:

$$J_A = u_2'\left[1 + \frac{u_0+\alpha_0}{u+u_2'}\right]P(0,A) \tag{A15}$$

and

$$J_B = \alpha_2'\left[1 + \frac{u_0+\alpha_0}{u+\alpha_2'}\right]P(0,B). \tag{A16}$$

These expressions lead directly to Eqs. (32) and (33) in the main text.

It is also important to consider the ratio of stationary probability functions, and from the above expressions, we derive

$$\frac{P(0,A)}{P(0,B)} = \frac{u_0}{\alpha_0}\frac{\left[\frac{u(\alpha_2'+\beta_2')+\alpha_1'\alpha_2'}{\alpha_1'(u_0+\alpha_0)} + \frac{(u+\alpha_1')\alpha_2'}{\alpha_1'(u+\alpha_2')}\right]}{\left[\frac{u(u_2'+w_2')+u_1'u_2'}{u_1'(u_0+\alpha_0)} + \frac{(u+u_1')u_2'}{u_1'(u+u_2')}\right]}. \tag{A17}$$

From this equation, we obtain Eq. (34) in the main text after substituting the explicit expressions for the transition rates.

2. $N = 2$ channels: The special site is at the entrance

The master equations for this system are given by

$$\frac{dP(0,0;t)}{dt} = w_1'P(A,0;t) + \beta_1'P(B,0;t) + u[P(0,A;t) + P(0,B;t)] - (u_0'+\alpha_0')P(0,0;t), \tag{A18}$$

$$\frac{dP(A,0;t)}{dt} = u_0' P(0,0;t) + w_2' P(0,A;t) + u[P(A,A;t)P(A,B;t)] - (u_1' + w_1')P(A,0;t), \quad \text{(A19)}$$

$$\frac{dP(B,0;t)}{dt} = \alpha_0' P(0,0;t) + \beta_2' P(0,B;t) + u[P(B,B;t) + P(B,A;t)] - (\alpha_1' + \beta_1')P(B,0;t), \quad \text{(A20)}$$

$$\frac{dP(0,A;t)}{dt} = u_1' P(A,0;t) + w_1' P(A,A;t) + \beta_1' P(B,A;t) - (u_0 + \alpha_0 + w_2' + u)P(0,A;t), \quad \text{(A21)}$$

$$\frac{dP(0,B;t)}{dt} = \alpha_1' P(B,0;t) + \beta_1' P(B,B;t) + w_1' P(A,B;t) - (u_0 + \alpha_0 + \beta_2' + u)P(0,B;t), \quad \text{(A22)}$$

$$\frac{dP(A,A;t)}{dt} = u_0' P(0,A;t) - (u + w_1')P(A,A;t), \quad \text{(A23)}$$

$$\frac{dP(B,A;t)}{dt} = \alpha_0' P(0,A;t) - (u + \beta_1')P(B,A;t), \quad \text{(A24)}$$

$$\frac{dP(A,B;t)}{dt} = u_0' P(0,B;t) - (u + w_1')P(A,B;t), \quad \text{(A25)}$$

$$\frac{dP(B,B;t)}{dt} = \alpha_0' P(0,B;t) - (u + \beta_1')P(B,B;t). \quad \text{(A26)}$$

Solving these equations at large times produces the following relations for the stationary-state probability functions:

$$P(A,B) = \frac{u_0'}{u + w_1'} P(0,B), P(B,A) = \frac{\alpha_0'}{u + \beta_1'} P(0,A), \quad P(A,A) = \frac{u_0'}{u + w_1'} P(0,A), P(B,B) = \frac{\alpha_0'}{u + \beta_1'} P(0,B) \quad \text{(A27)}$$

and

$$P(A,0) = \left[\frac{u + w_2'}{u_1'} + \frac{uK}{u_1'}\right] P(0,A), \quad \text{(A28)}$$

$$P(B,0) = \left[\frac{u + \beta_2'}{\alpha_1'} + \frac{uK}{\alpha_1'}\right] P(0,B), \quad \text{(A29)}$$

where an auxiliary function K is defined as

$$K \equiv \frac{\alpha_0'}{u + \beta_1'} + \frac{u_0'}{u + w_1'}. \quad \text{(A30)}$$

From Eq. (A18), we also obtain that

$$P(0,0) = \left[\frac{u\alpha_1' + w_1'(u + \beta_2')}{\alpha_1'(u_0' + \alpha_0')} + \frac{uw_1'K}{\alpha_1'(u_0' + \alpha_0')}\right] P(0,A) + \left[\frac{uu_1' + \beta_1'(u + w_2')}{u_1'(u_0' + \alpha_0')} + \frac{u\beta_1'K}{u_1'(u_0' + \alpha_0')}\right] P(0,B). \quad \text{(A31)}$$

Using these results in Eqs. (43) and (44) produces

$$J_A = u(K+1)P(0,A), \quad J_B = u(K+1)P(0,B). \quad \text{(A32)}$$

This is what was utilized in Eqs. (32) and (33) in the main text. In addition, one can calculate the important ratio of the probability functions,

$$\frac{P(0,A)}{P(0,B)} = \frac{\frac{\beta_1'\beta_2'}{\alpha_0'\alpha_1'} + \frac{(\alpha_1' + \beta_1')u(K+1)}{\alpha_0'\alpha_1'} + \frac{u(\beta_1' - w_1')}{(u+\beta_1')(u+w_1')}}{\frac{w_1'w_2'}{u_0'u_1'} + \frac{(u_1' + w_1')u(K+1)}{u_0'u_1'} + \frac{u(w_1' - \beta_1')}{(u+\beta_1')(u+w_1')}}. \quad \text{(A33)}$$

This equation leads directly to Eq. (47).

[1] J. Rehbein and B. K. Carpenter, Phys. Chem. Chem. Phys. **13**, 20906 (2011).
[2] C. Meloan, *Chemical Separations: Principles, Techniques, and Experiments* (Wiley Interscience Publication, New York, 1999).
[3] H. Lodish *et al.*, *Molecular Cell Biology*, 4th ed. (Scientific American Books, New York, 1995).
[4] Y. Caspi, D. Zbaida, H. Cohen, and M. Elbaum, Nano Lett. **8**, 3728 (2008).
[5] S. B. Lee, D. T. Mitchell, L. Trofin, T. K. Nevanen, H. Soderlund, and C. R. Martin, Science **296**, 2198 (2002).
[6] P. Kohli, C. Harrell, Z. Cao, R. Gasparac, W. Tan, and C. R. Martin, Science **305**, 984 (2004).
[7] S. M. Iqbal, D. Akin, and R. Bashir, Nat. Nanotechnol. **2**, 243 (2007).
[8] J. Cichelli and I. Zharov, J. Am. Chem. Soc. **128**, 8130 (2006).
[9] M. M. Mohammad, S. Prakash, A. Matoushek, and L. Movileanu, J. Am. Chem. Soc. **130**, 4081 (2008).
[10] T. Chou, J. Chem. Phys. **110**, 606 (1999).
[11] A. M. Berezhkovskii, M. A. Pustovoit, and S. M. Bezrukov, J. Chem. Phys. **116**, 9952 (2002).
[12] A. M. Berezhkovskii and S. M. Bezrukov, Chem. Phys. **319**, 342 (2005).
[13] A. B. Kolomeisky, Phys. Rev. Lett. **98**, 048105 (2007).
[14] A. B. Kolomeisky and K. Uppulury, J. Stat. Phys. **142**, 1268 (2011).
[15] A. Zilman, Biophys. J. **96**, 1235 (2009).
[16] A. Zilman, S. Di Talia, T. Jovanovic-Talisman, B. T. Chait, and M. P. Rout, PLoS Comput. Biol. **6**, e1000804 (2010).
[17] W. R. Bauer and W. Nadler, PLoS One **5**, e15160 (2010).
[18] S. K. Bhatia, M. R. Bonilla, and D. Nicholson, Phys. Chem. Chem. Phys. **13**, 15350 (2011).